

**2017 NDIA GROUND VEHICLE SYSTEMS ENGINEERING AND TECHNOLOGY  
SYMPOSIUM  
AUTONOMOUS GROUND SYSTEMS (AGS) TECHNICAL SESSION  
AUGUST 8–10, 2017; NOVI, MICHIGAN**

**IMPROVING THE FUEL ECONOMY OF CLASS 8 MILITARY VEHICLES USING A  
SMART CRUISE CONTROL ALGORITHM**

**Phillip Sharer**  
**Aymeric Rousseau**  
**Dominik Karbowski**  
**Daliang Shen**  
Systems Modeling & Control  
Argonne National Laboratory  
Argonne, IL

**Scott Heim**  
**Kevin Mark Gonyou**  
**Denise Rizzo**  
Tank Automotive Research and  
Development Center (TARDEC)  
Warren, MI

**Adam Ragatz**  
**Jeff Gonder**  
**Robert Prohaska**  
National Renewable Energy  
Laboratory  
Golden, CO

**Jae Song**  
DCSCorp  
Alexandria, VA

**ABSTRACT**

*Connected and automated vehicles (CAVS) have the potential to improve fuel economy by changing the way vehicles are driven. Fuel economy can be improved through a wide range of technologies, many of which do not require Level 5 automation. One of the most promising technologies is a smart cruise control that uses a speed-matching algorithm to account for fuel economy. Accounting for fuel economy in the algorithm leads to different driving behavior than simply matching the driver-entered set speed. This paper describes how such a smart cruise control could be applied to a class 8 vehicle both in simulation and in the actual vehicle on a closed test track. It evaluates the algorithm and describes the correlation procedure used to calibrate the model using test data from the vehicle.*

**INTRODUCTION**

Connected and automated vehicles (CAVS) have the potential to improve fuel economy by changing the way vehicles are driven. Fuel economy can be improved through a wide range of technologies, many of which do not require Level 5 automation. One of the most promising technologies is smart cruise control that uses an algorithm to account for

fuel economy, leading to different driving behavior than simply matching the driver-entered set speed. The first iteration of such a smart cruise controller in this study was a heuristic control that improved fuel economy by choosing an optimal set speed for the vehicle within a desired tolerance band. It also adjusted the set speed based upon grade information along the route. The general

UNCLASSIFIED: Distribution Statement A. Approved for public release; distribution is unlimited.



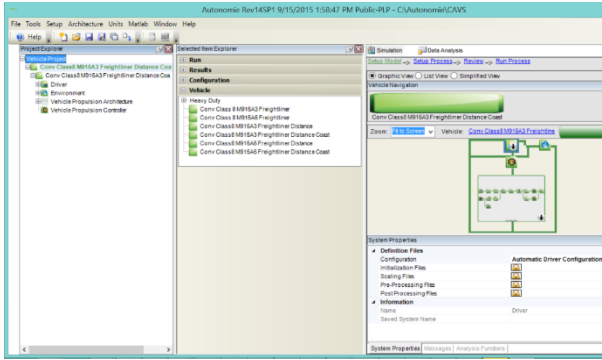


**Figure 2:** Autonomie REV15SP1 User Interface

## VEHICLES

The purpose of this paper is to demonstrate how fuel economy can be improved if the stock autonomous vehicle control strategy was modified to account for fuel economy. The way a human drives has a considerable effect on fuel economy. Aggressive driving leads to poor fuel economy. Having a control algorithm drive instead of a human affords us the opportunity to optimize driving behavior for fuel economy. This study used two Class 8 vehicles: the M915 A3 and the M915 A5 Line Haul. Both of these vehicles were outfitted with the Autonomous Mobility Applique System (AMAS) developed by Lockheed Martin. The AMAS system provides driver warning/driver assist and leader-follower capabilities; however, the AMAS control was not designed with fuel conservation as a goal. For instance, when in follower mode, the vehicle aggressively applies engine torque and brake to maintain a fixed gap distance. By smoothing the engine torque behavior and allowing more play in gap distance, the vehicle fuel economy could be improved. In addition, if the vehicle acceleration could be slowed when resuming motion after a stop, the fuel economy could be improved. The idea is to focus on different aspects of vehicle control and smooth out the system response so that aggressive driving is replaced with slower, smoother, more fuel-

efficient driving. Because this control was implemented in the actual vehicles, only two specific modes were selected to improve. Both involved the cruise control functionality of the vehicles.

The first control improvement occurs when initially setting the vehicle speed. When the vehicle cruise speed was set, instead of driving the exact set speed, the smart cruise picked the most efficient vehicle speed within -specified bounds of the set speed. The new speed had to be within specified bounds of the original set speed or the AMAS system would register a fault condition. In addition to adjusting the vehicle speed to obtain a better fuel economy, a route-based, look-ahead control was also considered. That is, when the controller detected an approaching change in grade, it would select a new set speed for the vehicle in order to improve the vehicle's overall fuel economy over the route.

The second control improvement occurs when returning to the previous set speed after a stop. This acceleration from stop to set speed was reduced to provide a more gradual acceleration.

We focused on these two modes of operation during this first phase of vehicle controller improvements. The ultimate goal is to improve all modes of autonomous driving, but this will happen during later phases.

## SMART CRUISE

A smart cruise control was developed to replace the stock cruise control of the vehicle.

UNCLASSIFIED

Improving the Fuel Economy of Class 8 Military Vehicles Using a Smart Cruise Control Algorithm, Sharer et al. 2017

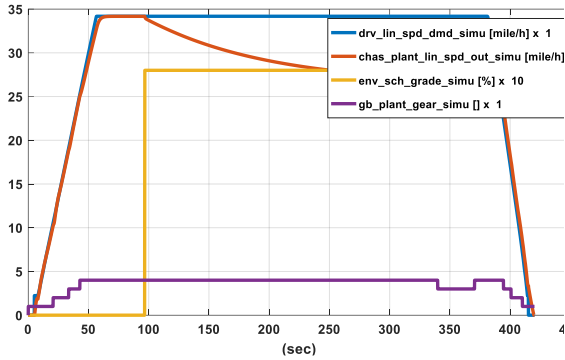


**Figure 3: Modifying the Set Speed for Better Fuel Economy**

The main goal for this first phase of the project was to collect data, refine the vehicle model, and use the refined vehicle model to develop a model predictive controller for the full platoon operation, which would be part of the second phase. However, for this initial phase of the project, it was desirable to provide a smart cruise controller that could improve fuel economy, but be a simpler heuristic controller that would be easy to implement in the vehicle and would override the default functionality of the AMAS. The controller is described below.

The basic controller is a PI controller (see Equation 1) with a  $K_p$  and  $K_i$  set based on the specific vehicle characteristics, such as vehicle mass, of the A3 or A5. Appropriate values were determined in simulation by running an optimization on the model:

$$T_{dmd} = K_p(V_{target} - V) + K_i \int (V_{target} - V) dt \quad (1)$$

Note that all variables in this equation and all following equations are defined in a table at the end of this paper.

Once the  $K_p$  and  $K_i$  values were known, we had to determine a method for predicting the

target speed that gives the best fuel economy, that is, the target speed that minimizes the following cost function:

$$V^* = \arg \min_V \int_T \dot{m}_{fuel}(V, \theta(t)) dt \quad (2)$$

We can determine the fuel mass flow rate by starting with the road load at the wheel and projecting it through the powertrain to the engine:

$$T_{dmd} = R_{wheel}(ma + mg(C_{rr0} + C_{rr1}V) \cos(\theta) + \dots + \frac{1}{2} \delta_{air} A C_d V^2 + mg \sin(\theta)) \quad (3)$$

Next, the torque demand at the engine can be projected through the transmission ratios and efficiencies to the engine:

$$T_{eng} = \frac{T_{dmd}}{\eta_{fd} \eta_{trans} R_{fd} R_{trans} (N_{gear})} \quad (4)$$

The wheel speed can also be projected through the transmission ratios to obtain the engine speed:

$$\omega_{eng} = V \times \frac{R_{fd} R_{trans} (N_{gear})}{R_{wheel}} \quad (5)$$

The transmission ratio is dependent on the gear number, which was given by a lookup table; this number is essentially a function of normalized torque demand at the wheels and vehicle speed:

$$N_{gear} = Shift(T_{dmd}, V) \quad (6)$$

The fuel rate of the engine can be expressed as a function of engine torque and engine speed:

UNCLASSIFIED

Improving the Fuel Economy of Class 8 Military Vehicles Using a Smart Cruise Control Algorithm, Sharer et al. 2017

$$\dot{m}_{fuel} = f(T_{eng}, w_{eng}) \quad (7)$$

Now Equation 3 can be inserted into Equation 4 and 6. Likewise, Equations 4 and 5 can be inserted into Equation 7 to produce an expression for the fuel rate in terms of the vehicle speed, grade and gear number:

$$\dot{m}_{fuel} = f(V, \theta, N_{gear}) \quad (8)$$

Substituting Equation 6 into Equation 8 produces the desired expression for fuel mass flow rate appearing in Equation 2. That is, assuming that the vehicle acceleration is negligible. Using this expression and assuming that the vehicle speed must be within a tolerance of the set speed (the speed set by the driver when enabling the cruise control), we can create a lookup table. That is, the additional constraint is as follows:

$$V_{driver} - \Delta V < V^* < V_{driver} + \Delta V \quad (9)$$

Basically, for a given set speed and grade, an optimum point was found within the tolerance and used as the alternative target speed in the controller map [2-4].

### CONTROLLER ADAPTED FOR HIL/SIL TEST BENCH

To use the smart cruise control in the HIL/SIL setup and within the test vehicle, the controller first had to (1) communicate via UDP and (2) run in real time. Both criteria were satisfied using the Simulink Desktop Real-time toolbox from Mathworks. This toolbox provides a real-time kernel that executes a Simulink diagram in real time. The UDP communication was provided through the UDP blockset that comes as part of the Simulink Desktop Real-time toolbox. An example is shown in Figure 4.

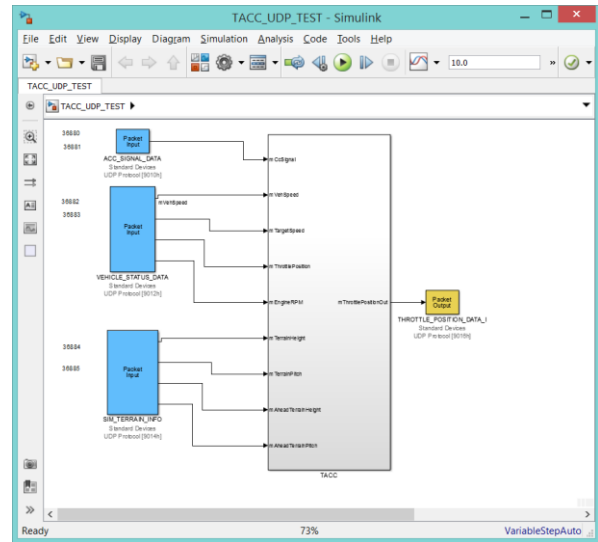


**Figure 4:** Top-Level Smart Cruise Control Diagram Showing UDP Interface

The controller ran in real time at a rate of 100 Hz on a laptop. The controller and the vehicle exchanged three input UDP packets and one output UDP packet. These packets are described in Tables 1, 2, 3, and 4:

**Table 1:** Input UDP Packet Vehicle Status

Data in Packet	Description
Vehicle Speed	Current speed of the vehicle
Target Speed	Desired speed of the vehicle (cruise control target set speed)
Engine Speed	Current engine speed
Engine Command	Current engine command
Packet Index	Packet index to order packets

**Table 2:** Input UDP Packet Cruise On

Data in Packet	Description
----------------	-------------

UNCLASSIFIED

Improving the Fuel Economy of Class 8 Military Vehicles Using a Smart Cruise Control Algorithm, Sharer et al. 2017

Engage	Tells controller when cruise control is turned on
--------	---

**Table 3:** Input UDP Packet Terrain Info

Data in Packet	Description
Terrain Pitch	Current grade

**Table 4:** Output UDP Packet Engine Command

Data in Packet	Description
Engine Command	0 to 100 percent engine command

### CONTROLLER IN VEHICLE

When testing the controller in the vehicle, constraints were added to ensure that the additional controller logic did not throw a fault. One of these constraints required maintaining the packet order, so a packet index had to be added to the input engine command packet, which was then passed through to the outgoing engine command packet. Initially, there were also other constraints on the magnitude of the engine command signal. Because the AMAS control was still active in the vehicle, but being bypassed, the control signal generated by the smart cruise had to fall within certain bounds of the original AMAS signal; otherwise, the system detected a fault condition. Work had to be performed to turn off this constraint to allow more freedom in the commanded engine torque.

### TEST DATA COLLECTION

Test data was collected from three sources. First, data was collected from the onboard vehicle J1939 CAN network. This set of signals included engine torque, engine speed, engine command, engine temperature, brake pedal percent, current gear, torque converter lockup state, and engine fuel rate, in addition to many other signals. Second, data was collected from a series of analog sensors.

This set of signals included fan speed, radiator in and out temperatures, and a few other signals. In some cases, both an analog sensor and CAN data was available. Finally, fuel rate data was collected from a special fuel rate measurement system spliced into the fuel line of the vehicle. This measurement allowed high-fidelity real-time measurement of the fuel rate. All of this data was collected and uploaded to a secure site using cellular network connectivity.

The A3 and A5 were both tested at the Aberdeen proving grounds on the Automotive Technology Evaluation Facility (ATEF) route and the Churchville C route. The ATEF route is a 4.5-mile circuit on level ground. The test was performed at a set speed of 50 mph in straight portions of the track and at 40 mph in the curved portions of the track. The test was repeated on the gravel loop of the track, which travels alongside the paved track. The Churchville C is a hilly track, 2.4 miles long, with a maximum grade of about 15%. Each track was tested several times. The driver completed a baseline run, along with runs with the AMAS controller and the smart cruise controller. They drove around 230 laps in total, over a period of four days.

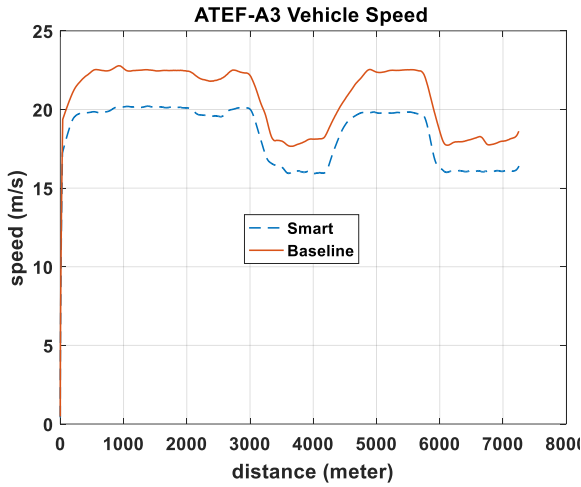
### TEST DATA ANALYSIS

We compared the baseline test driven by a human to the test using smart cruise. The following figures show smart cruise was able to improve fuel economy on the ATEF cycle.

Because the ATEF route is on level ground, the only method available to improve fuel economy there was to choose a more efficient vehicle speed at which to drive the vehicle. Figure 5 shows that smart cruise consistently chose a slower speed at which to drive the vehicle.

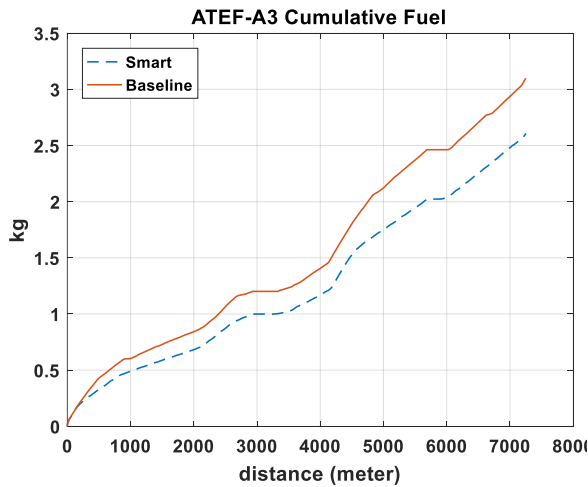
UNCLASSIFIED

Improving the Fuel Economy of Class 8 Military Vehicles Using a Smart Cruise Control Algorithm, Sharer et al. 2017



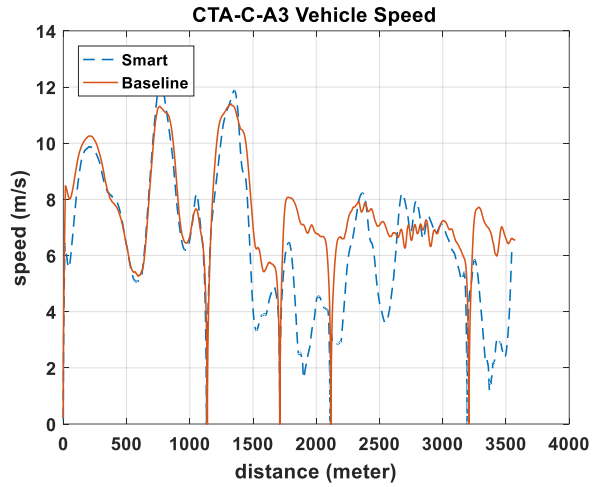
**Figure 5:** ATEF Vehicle Speed: Smart vs. Baseline

Figure 6 shows significant fuel savings from driving the vehicle slower. Even though this behavior can be easily replicated by a human driver, this exercise still demonstrates the concept of overriding the default cruise control with different logic to maximize the vehicle’s fuel economy.



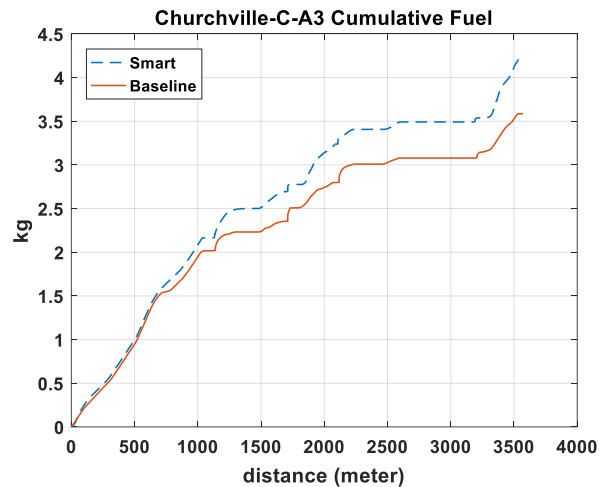
**Figure 6:** ATEF Cumulative Fuel Use: Smart vs. Baseline

Figure 7 illustrates the same operation. The smart cruise control chose to operate the vehicle at a lower vehicle speed.



**Figure 7:** Churchville-C Vehicle Speed: Smart vs. Baseline

However, in this case the strategy does not result in improved fuel economy; it leads to worse fuel economy. Figure 8 shows the mass of fuel consumed has increased over the lap.



**Figure 8:** Churchville-C A3 Cumulative Fuel Use: Smart vs. Baseline

Figure 9 shows that the fuel rate is significantly higher for the smart cruise than for the baseline around the 700<sup>th</sup> meter on the lap.

UNCLASSIFIED

Improving the Fuel Economy of Class 8 Military Vehicles Using a Smart Cruise Control Algorithm, Sharer et al. 2017

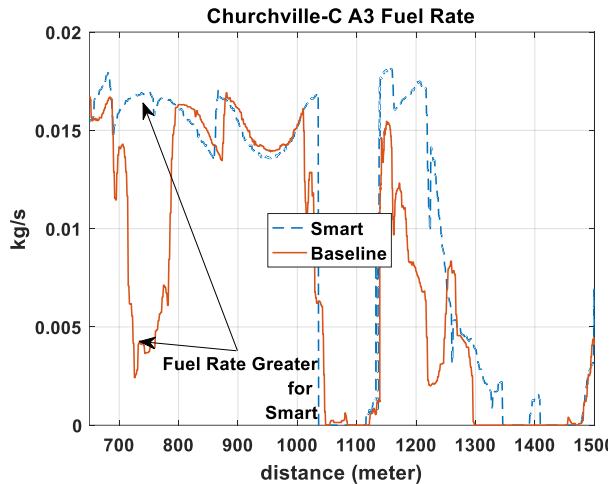


**Figure 9:** Churchville-C A3: Smart vs. Baseline, Fuel Rate Event 1

Figure 10 shows that the higher fuel rate is related to a greater engine torque demand rather than a less-efficient operating point of the engine. Why is the demand for the smart cruise so high, when the demand for the baseline is much lower?

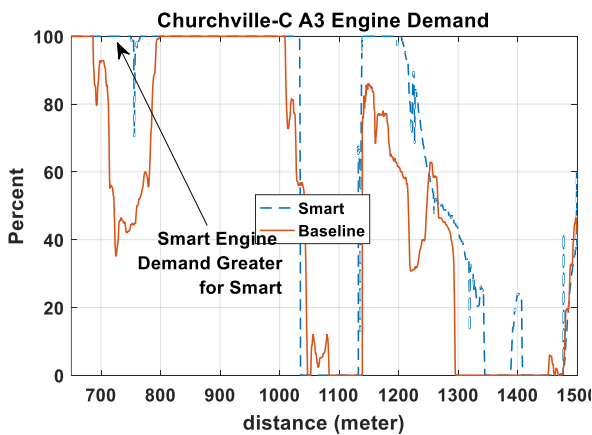


**Figure 10:** Churchville-C A3: Smart vs. Baseline, Engine Demand Event 1

Figure 11 shows that the vehicle is beginning to head downhill. This indicates that the controller was not receiving the necessary grade information to make an accurate determination of the required load on the engine. It was later confirmed that this was indeed the case. The controller had

issues computing the grade from the elevation data coming off of the CAN because the data was noisier than expected and intermittently unavailable.

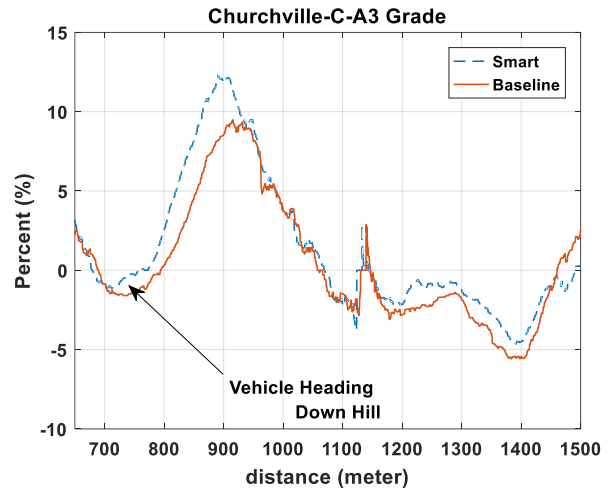


**Figure 11:** Churchville-C A3: Smart vs. Baseline, Grade Event 1

Figure 12 shows another mode on the Churchville course for which the fuel rate was higher for the smart cruise controller than for the baseline.

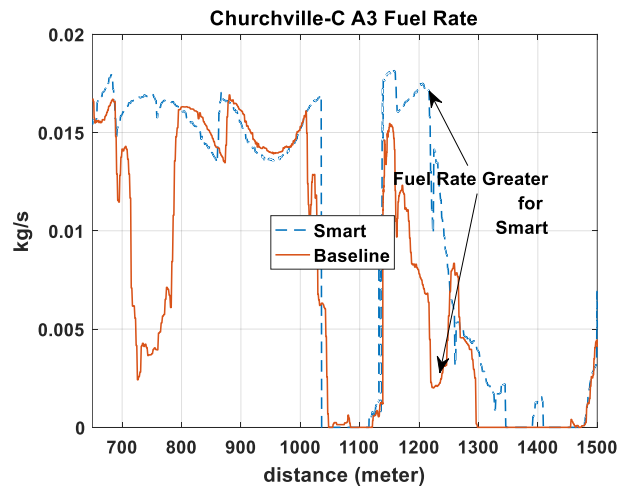
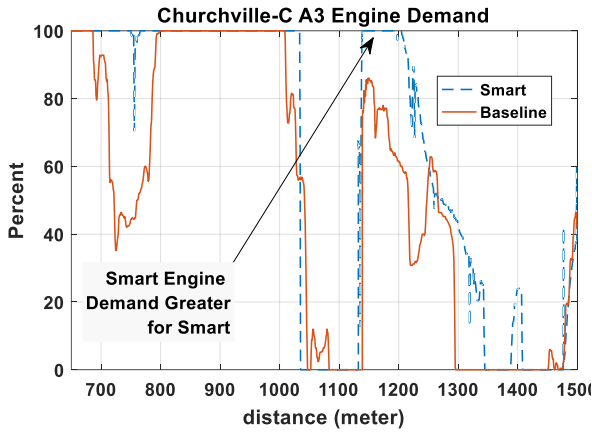


**Figure 12:** Churchville-C A3: Smart vs. Baseline, Fuel Rate Event 2

UNCLASSIFIED

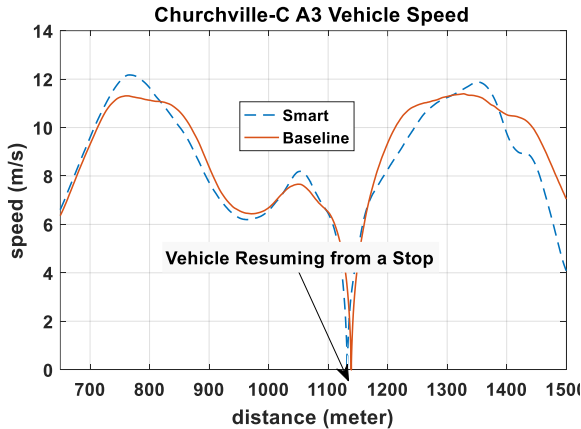
Improving the Fuel Economy of Class 8 Military Vehicles Using a Smart Cruise Control Algorithm, Sharer et al. 2017

Figure 13 shows that this occurs because the engine demand again is much higher for the smart cruise.



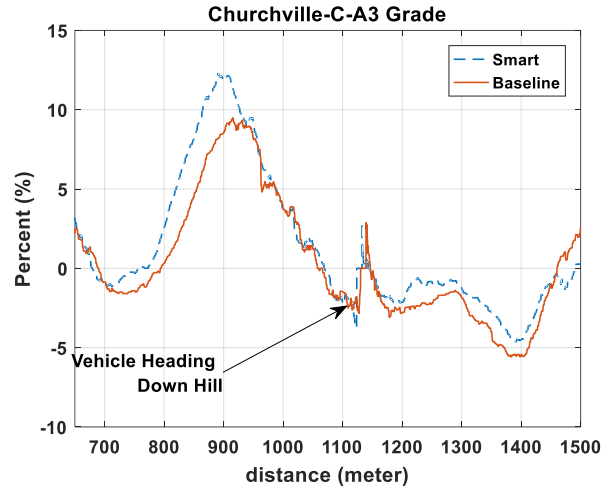
**Figure 13:** Churchville-C A3: Smart vs. Baseline, Engine Demand Event 2

Figure 14 shows that the event occurs when the vehicle is accelerating from a stop.



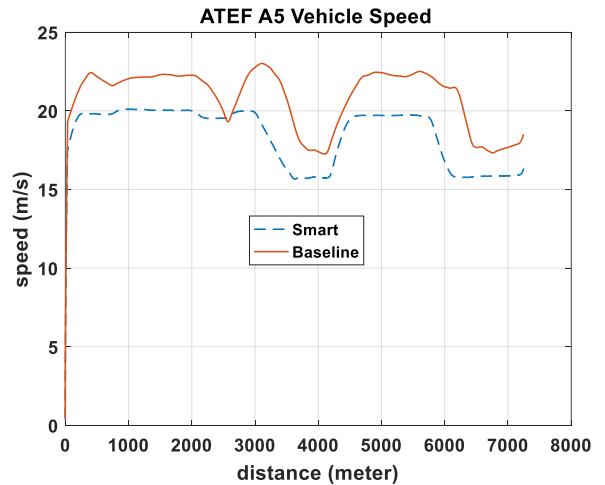
**Figure 14:** Churchville-C A3: Smart vs. Baseline, Vehicle Speed Event 2

Figure 15 shows that the stop occurs on a downhill portion of the lap. Yet again, it seems like the controller, unaware of grade, is overcompensating and demanding too much torque from the engine.



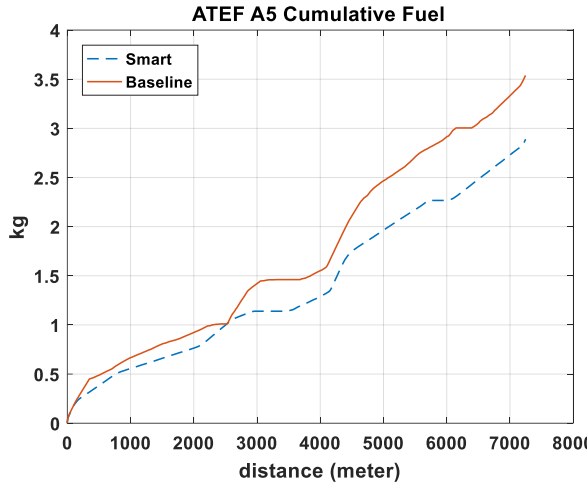
**Figure 15:** Churchville-C A3: Smart vs. Baseline, Grade Event 2

Figure 16 shows the behavior of the smart cruise compared to the baseline for the A5. It exhibited the same driving behavior as for the A3. The smart cruise drove the vehicle at a slower speed.



**Figure 16:** ATEF A5: Smart vs. Baseline, Vehicle Speed

Figure 17 shows the total fuel consumed.



**Figure 17:** ATEF A5: Smart vs. Baseline, Cumulative Fuel Use

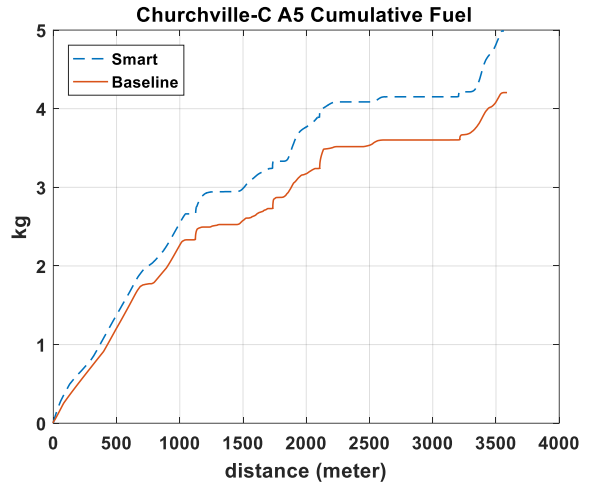


**Figure 19:** Churchville-C A5: Smart vs. Baseline, Vehicle Speed

Figures 18 and 19 compare the smart cruise with the baseline human driver for the A5 on the Churchville C cycle. As for the A3, the smart cruise consumed more fuel because of difficulties with responding to grade.

Another factor which could have lead to worse fuel economy was the lack of control over the gear selection. When in smart cruise mode, the AMAS control still determined the desired gear which could have impaired the smart cruise controller. Having control over the gear selection could have allowed the controller to improve the fuel economy of the vehicle.

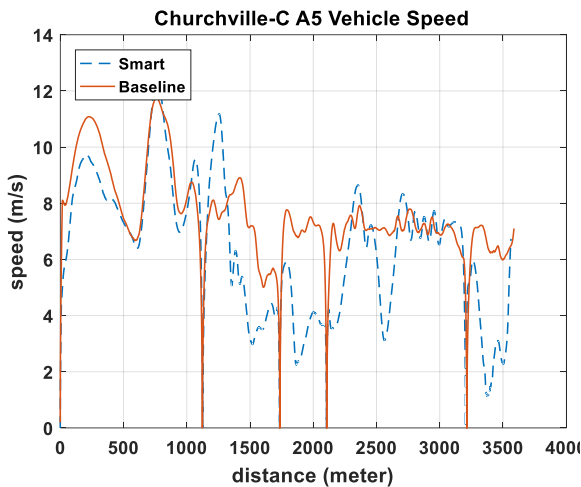


**Figure 18:** ATEF A5: Smart vs. Baseline, Vehicle Speed

**MODEL CORRELATION**

One of the main goals of this first phase of testing was to use the test data from the vehicles to refine the models, so the revised models could be used in the next phase of control development. Therefore, the Autonomie vehicle models for both the A3 and the A5 were updated and correlated with the test data. The modifications to the vehicle models are described next.

*Accounting for Wind*

The wind speed was recorded during the test and used it in place of the vehicle speed to calculate the air dynamic losses. It was assumed that the recorded wind speed represented the airflow across the vehicle.

UNCLASSIFIED

Improving the Fuel Economy of Class 8 Military Vehicles Using a Smart Cruise Control Algorithm, Sharer et al. 2017

***Gear Shifting***

There were differences in the gear shifting between the test data and the simulation. These differences were primarily due to engine braking events that would trigger a downshift in the vehicle. To overcome these differences in gear shifting, the measured gear from the vehicle was injected into the model, so that the rest of the losses in the vehicle model could be compared to the test data.

***Accessory Load***

The initial average mechanical accessory load was not sufficient for these vehicles and their loading. The fan would turn on frequently to cool the vehicle. To get a better estimate of the mechanical accessory losses, we analyzed each lap to identify conditions when the vehicle was stopped but the engine was still producing power. Using the value of the accessory load while the vehicle was stopped provided a better estimate for the fuel consumption. Figure 20 shows a distribution plot for the A3 mechanical accessory load while the vehicle is stopped during the ATEF cycle. Figure 21 shows the same plot for the A3 on the Churchville-C cycle. Because the Churchville-C cycle is more aggressive, the fan had to turn on more frequently to cool the engine. The air conditioner was also running continuously during the test.

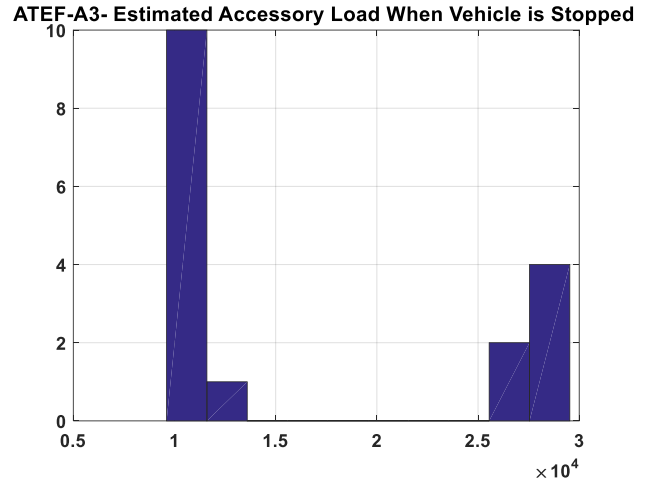


**Figure 20:** Mechanical Accessory Load Distribution on the ATEF for the A3

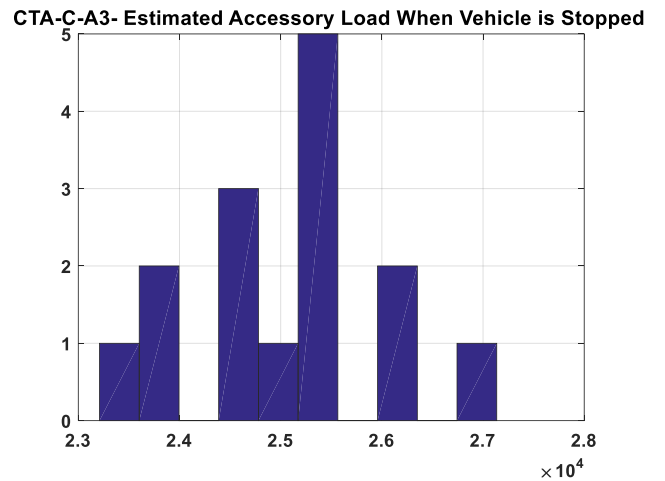


**Figure 21:** Mechanical Accessory Load Distribution on the Churchville-C for the A3

***Rolling Resistance***

The ATEF had both a paved and a gravel loop, while the Churchville-C only had a gravel loop. The gravel road surface changed the rolling resistance of the vehicle. To determine the rolling resistance on the gravel road, the model was first correlated on the paved road. The model developed from the paved road was then simulated on the gravel loop. The rolling resistance coefficient was then adjusted until the error between the test fuel consumption and the simulated fuel

UNCLASSIFIED

consumption was minimized. This procedure was repeated for each lap, and a histogram of rolling resistance coefficients was created. From this histogram, we obtained a weighted value representing the rolling resistance for the ATEF. We repeated this procedure for the Churchville-C. Figure 22 shows an example histogram computed from the lap data. A least-squares fit was also performed, but the optimization routine yielded a more reasonable value for the coefficient.

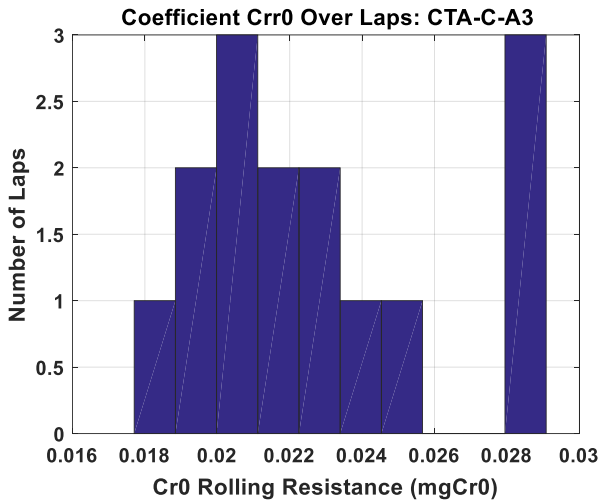


**Figure 22:** Estimated Rolling Resistance Coefficients for the Churchville-C

**Engine Map**

A new engine map was created from the test data. The fuel rate data from a selection of laps, from both the ATEF and Churchville-C, were binned as a function of torque and speed. Next, the Mathworks algorithm griddata was used to fit a parametric surface to the data. This surface was smoothed using a Gaussian filter to remove any jagged edges and high-frequency noise. The new engine map yielded a 4 to 5% improvement in the fuel economy prediction.

**Correlation Results**

After the model was calibrated using the test data, while still preventing over fitting, it

showed good correlation with the test data. Figure 23 shows this for the A3.

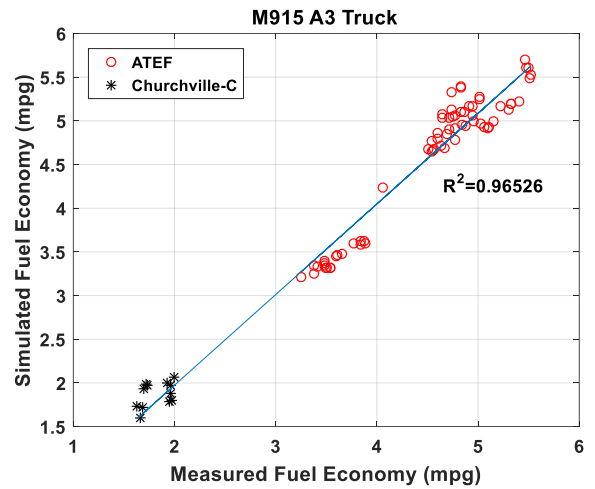


**Figure 23:** Correlation between Test Data and Simulation for the A3

Figure 14 shows the correlation between the simulation and the test data for the A5.

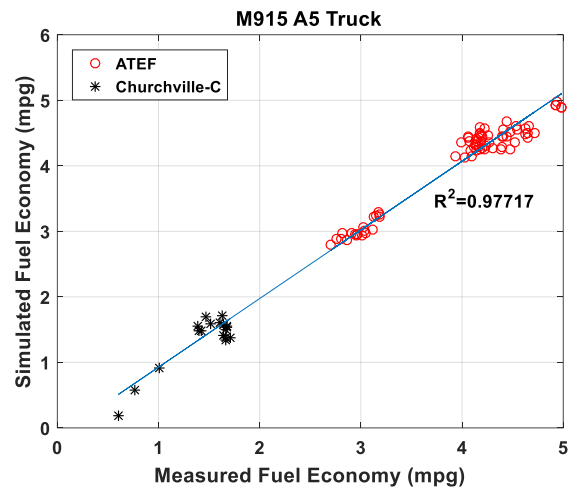
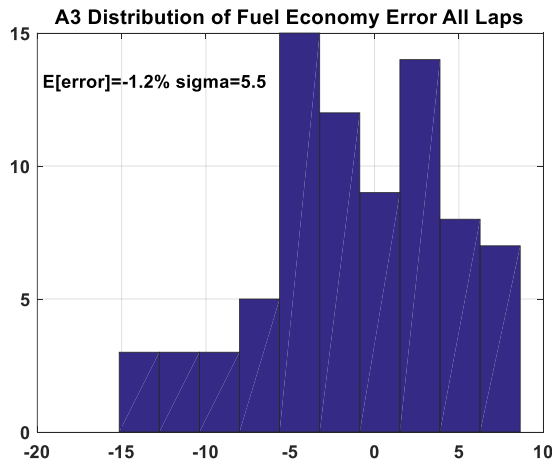


**Figure 24:** Correlation between Test Data and Simulation for the A5

Figure 25 shows a histogram of the percent error in fuel economy for the A3 vehicle. This histogram shows the percent difference between the simulated fuel economy and the measured fuel economy across all of the laps, both ATEF and Churchville-C. The mean

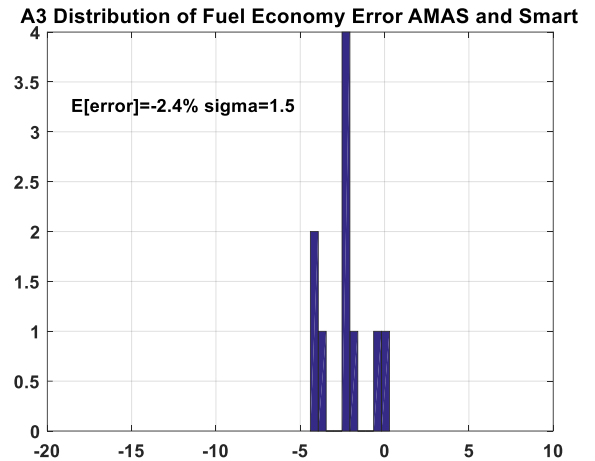
UNCLASSIFIED

percent error is about 1.2%, but the standard deviation of the percent error is 5.5% percent. This indicates that the percent error is spread out over a wide band, although the mean error of the simulation is small. The reason for this is threefold: lap-to-lap variability due to the human driver, variability in the surface conditions of the gravel road, and variability due to uncertainty in the grade.



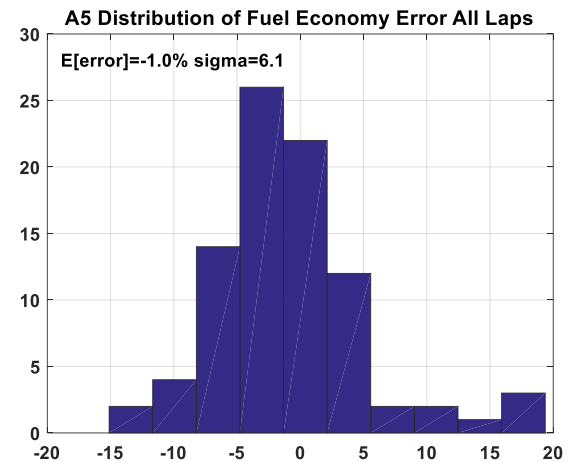
**Figure 25:** Histogram of Percent Fuel Economy Error for A3

Figure 26 is a histogram of percent error that illustrates the reduced variability in the percent error when considering only laps driven by the AMAS and smart cruise over flat, paved roads. In this case, the mean error indicates the result is still biased by -2.4%, but the standard deviation of the percent error has dropped significantly. This dramatic decrease in variability can be attributed to excluding the following three conditions: any lap driven by a human driver, any lap driven on a gravel road, and any lap with a variable grade.



**Figure 26:** Histogram of Percent Fuel Economy Error for A3 AMAS and Smart Laps

Figure 27 shows similar results for the A5. The mean error is low, but the variability is high.



**Figure 27:** Histogram of Percent Fuel Economy Error for A5

Figure 28 shows similar results when the analysis is limited to the AMAS or smart cruise on flat paved roads.

UNCLASSIFIED

Improving the Fuel Economy of Class 8 Military Vehicles Using a Smart Cruise Control Algorithm, Sharer et al. 2017

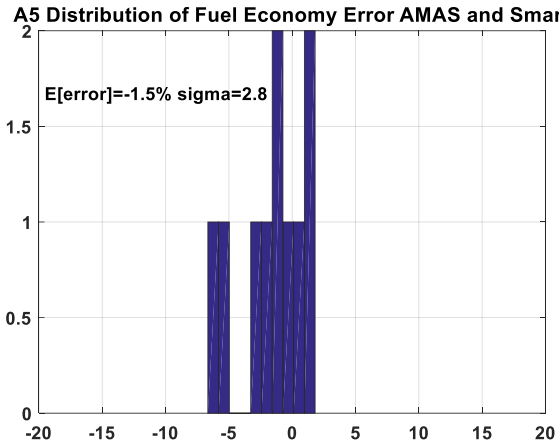


**Figure 28:** Histogram of Percent Fuel Economy Error for A3 AMAS and Smart Laps

The vehicle model calibrated using the test data is more accurate than the original model used to design the first phase of the smart cruise control. Even though the model was less accurate during the first iteration, it still enabled the controller development to proceed, yielding a controller that improved the fuel economy. We expect that this refined vehicle model, calibrated using the test data, will yield an even better controller for the second phase. Having a more accurate vehicle model will also make calibrating the controller in simulation easier, thereby reducing the overall calibration time in the vehicle.

### NEXT STEPS

The next steps of this project will involve using a distance horizon and creating a model predictive control (MPC) using the vehicle model correlated to the test data. Figure 29 shows how the MPC will look ahead and optimize fuel economy over the horizon [5].

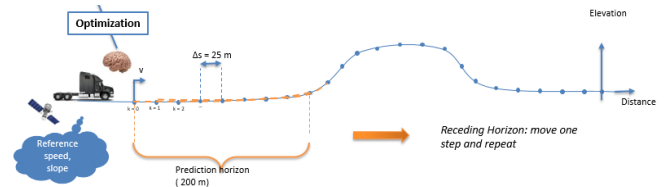


**Figure 29:** Model Predictive Controller over a Horizon

In addition, the vehicle will be tested as part of a convoy during the next round of vehicle testing.

### CONCLUSIONS

For this study, a smart cruise controller was developed and calibrated in simulation for two Class 8 trucks: a M915 A3 and a M915 A5. We then ran the smart cruise control as part of the HIL/SIL system and later used it in test vehicles on the ATEF and Churchville-C courses. Fuel economy improvement was demonstrated for the smart cruise control on the ATEF course. However, no fuel economy improvement was shown for the Churchville-C Course, primarily because of the limited availability of information about the route during testing. This issue will be addressed in future testing by providing a grade horizon up to 200 meters in front of the vehicle. The test data that was collected from this first round of testing was correlated with the vehicle models and used to improve the accuracy of the model. This will help in the development of the MPC.

### REFERENCES

- [1] S. Halbach et al. "Model Architecture, Methods and Interfaces for Efficient Math-Based Design and Simulation of Automotive Control Systems", SAE Technical Paper 2010-01-0241
- [2] A. Delorme et al. "Fuel Economy Potential of Advanced AMT eCoast Feature in Long-Haul Applications", SAE Technical Paper 2014-01-2324.

UNCLASSIFIED

Improving the Fuel Economy of Class 8 Military Vehicles Using a Smart Cruise Control Algorithm, Sharer et al. 2017

- [3] J. Wang and R. Longoria “Effect of Computational Delay on the Performance of a Hybrid Adaptive Cruise Control System”, SAE Journal of Vehicle Dynamics and Simulation, SAE Technical Paper 2006-01-0800.
- [4] H. Kim and K. Yi “Design of a Model Reference Cruise Control Algorithm”, SAE International Journal of Passenger Cars - Electronic and Electrical Systems, SAE Technical Paper 2012-01-0492.
- [5] Karbowski, D., Kim, N., Rousseau, A., “Route-Based Energy Management for PHEVs: A Simulation Framework for Large-scale Evaluation” EVS28, May 2015, Korea.

#### **CONTACT INFORMATION**

Phillip Sharer  
psharer@anl.gov

#### **ACKNOWLEDGEMENTS**

The authors acknowledge that funding for the work performed within the Autonomy-Enabled Fuel Savings for Military Vehicles project is provided by the Office of the Deputy Assistant Secretary of Defense for Operational Energy (ODASD [OE]) Operational Energy Capabilities Improvement Fund (OECIF) Program. TARDEC greatly appreciates the support it has received from the Director of Innovation and staff of ODASD (OE) within the Office of the Assistant Secretary of Defense for Energy, Installations & Environment.

#### **DISCLAIMER**

Reference herein to any specific commercial company, product, or service by trade name, trademark, manufacturer, or otherwise, does not necessarily constitute or imply its endorsement, recommendation, or favoring by the United States Government or the

Department of the Army (DoA). The opinions of the authors expressed herein do not necessarily state or reflect those of the United States Government or the DoA, and shall not be used for advertising or product endorsement purposes.

The submitted manuscript has been created by UChicago Argonne, LLC, Operator of Argonne National Laboratory (“Argonne”). Argonne, a U.S. Department of Energy Office of Science laboratory, is operated under Contract No. DE-AC02-06CH11357. The U.S. Government retains for itself, and others acting on its behalf, a paid-up nonexclusive, irrevocable worldwide license in said article to reproduce, prepare derivative works, distribute copies to the public, and perform publicly and display publicly, by or on behalf of the Government. The Department of Energy will provide public access to these results of federally sponsored research in accordance with the DOE Public Access Plan. <http://energy.gov/downloads/doe-public-accessplan>

UNCLASSIFIED

Improving the Fuel Economy of Class 8 Military Vehicles Using a Smart Cruise Control Algorithm, Sharer et al. 2017

**DEFINITIONS/ABBREVIATIONS**

$K_p$	Proportional gain for the PI controller
$K_i$	Integral gain for the PI controller
$V^*$	The vehicle speed which minimizes the cost
$\mathbf{V}$	The set of all admissible vehicle speeds
$V_{driver}$	The given set speed set by the driver
$V_{target}$	Target speed for the PI controller
$V$	Vehicle speed
$\Delta V$	Vehicle speed tolerance
$t$	Time
$T$	The time period over which the cost function is evaluated
$\omega_{eng}$	Engine speed
$T_{dmd}$	Torque demand at the wheels
$T_{eng}$	Torque at the engine
$\dot{m}_{fuel}$	The mass flow rate of the fuel
$C_{rr0}$	The first-order rolling resistance coefficient
$C_{rr1}$	The second order rolling resistance coefficient
$\theta$	Grade angle
$A$	Frontal area of the vehicle
$C_d$	Coefficient of drag
$\delta_{air}$	Air density
$g$	Acceleration due to gravity
$m$	Mass of the vehicle
$R_{wheel}$	Rolling radius of the wheel
$R_{fd}$	Ratio of the final drive
$R_{trans}$	Ratio of the transmission as a function of gear number
$N_{gear}$	Gear number
$\eta_{fd}$	Efficiency of the final drive
$\eta_{trans}$	Efficiency of the transmission

UNCLASSIFIED

Improving the Fuel Economy of Class 8 Military Vehicles Using a Smart Cruise Control Algorithm, Sharer et al. 2017